On the cause of abrupt vegetation collapse in North Africa during the Holocene: Climate variability vs. vegetation feedback

Zhengyu Liu,[1,2] Yi Wang,[1] Robert Gallimore,[1] Michael Notaro,[1] and I. Colin Prentice[3]

Received 3 September 2006; revised 18 October 2006; accepted 20 October 2006; published 23 November 2006.

[1] The abrupt desertification over the northern Africa in the mid-Holocene is studied in both a complex and a simple coupled climate-vegetation model. In contrast to the previous mechanism that relies on strong positive vegetation-climate feedback and the resulted multiple equilibria, we propose a new mechanism in which the abrupt desertification is caused by low frequency climate variability, rather than a positive vegetation-climate feedback. The implication of this new mechanism to modelling and observation is also discussed.

Citation: Liu, Z., Y. Wang, R. Gallimore, M. Notaro, and I. C. Prentice (2006), On the cause of abrupt vegetation collapse in North Africa during the Holocene: Climate variability vs. vegetation feedback, *Geophys. Res. Lett.*, *33*, L22709, doi:10.1029/2006GL028062.

1. Introduction

[2] One great abrupt environmental change event was observed in the northern Africa in the mid-Holocene, with a dramatic desertification occurred abruptly within centuries [*deMenocal et al.*, 2000] (Figure 1a). Although the general desertification tendency in the Holocene is known to be forced by the change of orbital forcing, it has remained poorly understood why this northern Africa desertification occurred so abruptly. Based on the study in a climate-vegetation model of intermediate complexity, *Claussen et al.* [1999] first proposed a mechanism that depends on a strong positive vegetation-climate feedback and the resulted multiple equilibria in the coupled climate-vegetation system [*Claussen*, 1997, 1998]. In their mechanism, the abrupt desertification is induced by an unstable transition from the green Sahara equilibrium state to the desert Sahara equilibrium state. However, it has remained unclear why the desertification did not occur abruptly in other similar intermediate complexity models [*Renssen et al.*, 2003; *Wang et al.*, 2005]. Here, the North African desertification is studied in a first transient Holocene simulation in a synchronously coupled general circulation atmosphere-ocean-vegetation model (Z. Liu et al., Simulating the transient evolution and abrupt change of Northern Africa atmosphere-ocean-terrestrial ecosystem in the Holocene, submitted to *Quaternary Science Reviews*, 2006, hereinafter referred to as Liu et al., submitted manuscript, 2006). Furthermore, a conceptual climate-ecosystem model is developed to highlight the mechanism of the abrupt desertification and to provide a unified view of the evolution of the vegetation-climate system. In particular, our study suggests a new mechanism for the abrupt desertification, in which the abrupt change is induced by low frequency climate variability, rather than a strong vegetation feedback and the associated multiple equilibrium.

2. The GCM Simulation

[3] The Holocene experiment is integrated in the fully coupled atmosphere-ocean-land model, FOAM-LPJ [*Gallimore et al.*, 2005], under the annually varying orbital forcing [*Berger*, 1978] for the last 6500 years. A detailed discussion of the simulation and a comparison with past climate records are given by Liu et al. (submitted manuscript, 2006). Here, we focus on the mechanism of the abrupt desertification in the southern Sahara. The simulated grassland collapses abruptly into a desert around 5000 years ago (Figure 1b), in good agreement with the abrupt increase of dust flux in the Atlantic (Figure 1a). In contrast to the abrupt vegetation collapse, however, the simulated rainfall decreases gradually (Figure 1c), with the decline around 5000 yr BP comparable with internal climate variability. Moreover, this precipitation decline is likely to be the cause, rather than the consequence, of the vegetation collapse. This is because the rainfall changes tend to precede vegetation changes, implying the absence of a significant positive vegetation feedback on rainfall over Northern Africa. Indeed, the cross-correlation between annual vegetation cover and annual precipitation shows a significant (at 95% level) positive peak decreasing from lag 0 to several years with precipitation leading, reflecting the strong precipitation forcing on vegetation. However, the correlation becomes insignificant when vegetation leads annual precipitation by one year, suggesting a lack of positive feedback of annual vegetation on rainfall [*Liu et al.*, 2006]. This lack of strong positive feedback of vegetation cover on rainfall is also confirmed with a sensitivity experiment in which the change of vegetation cover over southern Sahara from the mid-Holocene to the pre-industrial leads to an slight increase of rainfall (not shown). Consequently, the simulated vegetation collapse is unlikely to be caused by the vegetation feedback mechanism proposed by *Claussen et al.* [1999]. Instead, we show in a conceptual model below that this abrupt vegetation collapse is caused by the strong low frequency climate variability forcing.

3. The Conceptual Model

[4] Our conceptual climate-vegetation model is similar to *Brovkin et al.* [1998] with the addition of a stochastic climate forcing simulating the strong internal variability of precipitation [*Zeng and Neelin*, 2000; *Wang*, 2004]. Vegetation in

[1]Center for Climatic Research, University of Wisconsin-Madison, Madison, Wisconsin, USA.
[2]Earth Environmental Institute, Chinese Academy of Sciences, Beijing, China.
[3]Department of Earth Sciences, University of Bristol, Bristol, UK.

0094-8276/06/2006GL028062$05.00

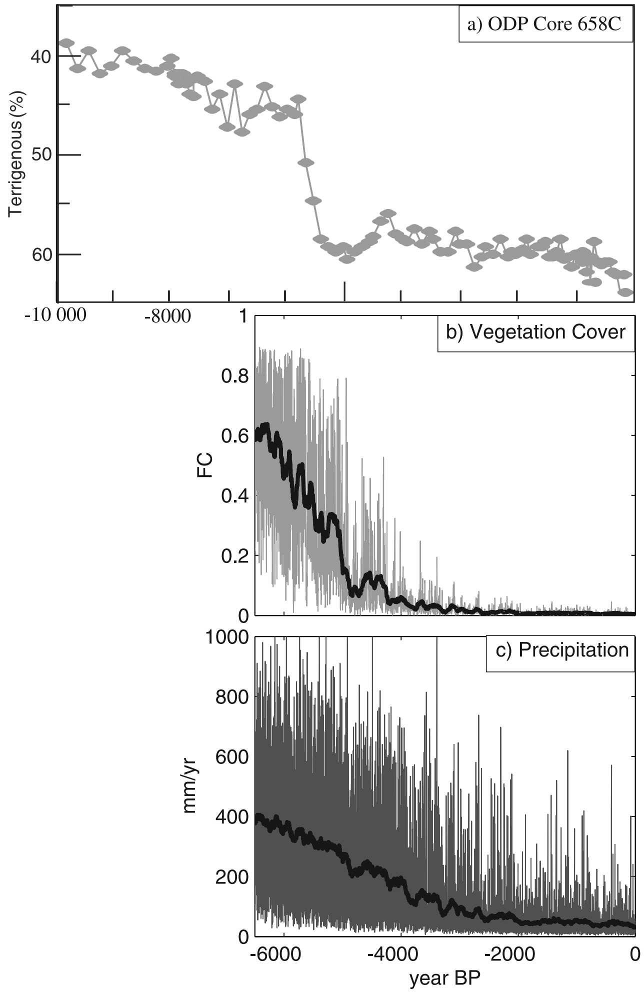

Figure 1. Time series of dust flux, vegetation, and precipitation. (a) Dust terrigenous record over the eastern North Atlantic at site 658C (20°N, 18°W) (adapted from *deMenocal et al.* [2000]); annual (b) total vegetation cover and (c) precipitation (mm/yr) in the southern Sahara (18–23°N, 11–36°E) in the transient FOAM-LPJ Holocene simulation. In Figures 1b and 1c, light thin lines are for annual data and heavy lines are for the 100-year running mean climatology.

the subtropical semi-desert area depends critically on water availability or soil moisture, which is represented crudely as proportional to the annual rainfall P. The vegetation cover V evolves as

$$dV/dt = [V_E(P) - V]/\tau, \tag{1}$$

where τ is the vegetation equilibrium time, taken as 5 years for the Sahara grasslands. The equilibrium vegetation model $V_E(P)$ assumes the form

$$V_E(P) = \begin{cases} 1 & P > P_{C2} \\ (P - P_{C1})/D_C & P_{C2} > P > P_{C1} \\ 0 & P < P_{C1} \end{cases} \tag{2}$$

Here, P_{C1} and P_{C2} are the lower and upper rainfall thresholds, respectively, and $D_C = P_{C2} - P_{C1} > 0$ is the precipitation range for the transition of equilibrium vegetation from the green state to desert state. Below, we use P_{C1} = 270 mm/yr and P_{C2} = 370 mm/yr to be consistent with the equilibrium solutions of our LPJ vegetation model (Figure 2); this is shown as the circles in Figures 3a and 4a.

[5] The equilibrium atmospheric precipitation model takes the form of

$$P_E(V) = P_d(t) + D_B V \tag{3}$$

with D_B as the vegetation feedback coefficient, and $P_d(t)$ as the background precipitation in the absence of vegetation. In the semi-desert region, rainfall has a strong internal variability independent of vegetation (Figure 1c). This internal variability is simulated as a stochastic forcing $P_N(t)$ into the total precipitation as

$$P(V,t) = \max\{P_E(V) + P_N(t), 0\} \tag{4}$$

An equilibrium coupled state can be identified as the intersection between the equilibrium vegetation $V_E(P)$ (in (2)) and equilibrium atmosphere $P_E(V)$ (in (3)) on the V-P plane (see crosses later in Figures 3a and 4a). One can show that instability and multiple equilibria exist only for a sufficiently strong positive vegetation feedback with $D_B > D_C$.

[6] Two cases will be discussed here: one with strong positive vegetation feedback (D_B = 150mm/yr, Figure 3a) and the other weakly positive vegetation feedback (D_B = 50 mm/yr, Figure 4a). These two cases are selected here mainly for their different stability properties, as will be discussed later. The gradual change of orbital forcing is simulated in the background precipitation as $P_d(t) = P_{d0}[1 - (t + 6500)/T]$, where P_{d0} is the background precipitation at −6500 yr and T is the period of interest. Here, T is taken as 3000 yr, because we are only interested in the period of abrupt change. Figures 3a and 4a (solid lines) show the equilibrium atmospheric states $P_E(V)$ at 6 time slices of years −6500, −5900, −5300, −4700, −4100 and −3500. The strong feedback case becomes unstable in the forcing range of $P_{C1} - (D_B - D_C) < P_d(t) < P_{C1}$. For example, the time slice at −5900 yr has three equilibria: an unstable intermediate

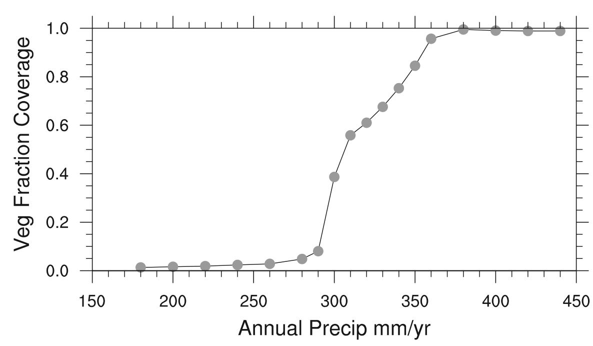

Figure 2. LPJ model equilibrium vegetation. Vegetation cover fraction as a function of annual precipitation simulated in the offline LPJ model in the southern Sahara region (18–23°N, 11–36°E). Each equilibrium state (dot) is obtained from a 100-yr integration of LPJ initialized from a bare ground. All the simulations are forced by the same mid-Holocene climatology of climate forcing from the Holocene experiment, except for the precipitation, which varies among integrations by varying the amplitude of rainfall's climatological annual cycle.

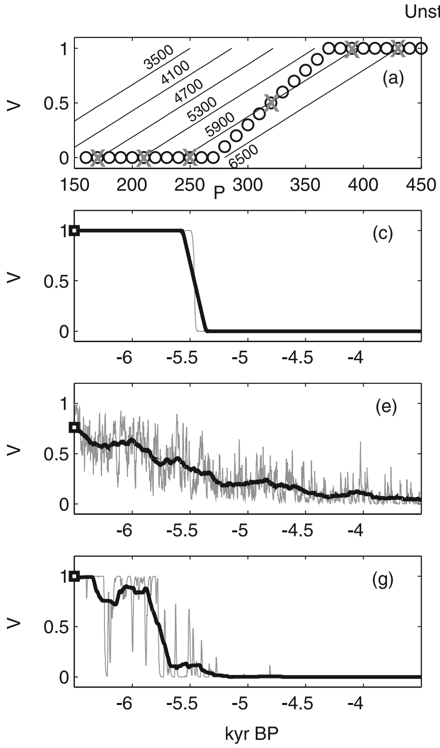

Figure 3. Vegetation-climate solution in the conceptual model for the strong feedback case (D_B = 150 mm/yr). (a) Equilibrium vegetation (circle), and 6 time slices of equilibrium atmosphere states (lines), and (b) their 6 corresponding stability potential functions $G(V)$. The time is marked on each line (with the negative sign omitted). In Figures 3a and 3b, the coupled equilibrium states are marked by crosses. (c and d) Temporal evolution under a slowly evolving background precipitation forcing (representing orbital forcing) for vegetation cover and for precipitation, respectively. (e and f) Same as Figures 3c and 3d but with the addition of a stochastic annual precipitation forcing of s.d. = 130 mm/yr. (g and h) Same as Figures 3e and 3f except that the annual stochastic precipitation forcing is low-pass filtered with a 10-year running mean. In Figures 3c–3h, the annual data (thin line) are plotted together with its 100-year running mean climatology (heavy line). In Figures 3d, 3f, and 3h, the two dash lines are the critical precipitation thresholds P_{C2} and P_{C1} for equilibrium vegetation. Figures 3c and 3d show an unstable collapse; the collapse is suppressed by a fast stochastic forcing in Figures 3e and 3f and is reactivated by a slow stochastic forcing in Figures 3g and 3h.

state ($V \approx 0.5$), a stable green state ($V = 1$) and a stable desert state ($V = 0$) (crosses in Figure 3a). The weak feedback case is always stable with a single equilibrium (crosses in Figure 4a). Following *Brovkin et al.* [1998], the stability of each equilibrium state can be seen in its potential function $G(V) = -\int_1^V \{V_E[P_E(V)] - V\}dV$ as shown in Figures 3b and 4b for the two cases. Each case shows 6 potential functions corresponding to the 6 times slices in Figures 3a and 4a. On each potential function curve, a maximum $G(V)$ peak represents an unstable equilibrium while a minimum $G(V)$ "well" represents a stable equilibrium. All the equilibrium states (crosses in Figures 3b and 4b) are stable as seen in the corresponding $G(V)$ wells, except for the strong feedback case at −5900 yr, in which an intermediate state (V = 0.5) becomes unstable as shown in a weak $G(V)$ peak in Figure 3b.

4. Vegetation Feedback and Vegetation Collapse

[7] Past studies focused on the collapse mechanism in the absence of climate variability. Figures 3c and 3d show the evolution of the vegetation and precipitation for the strong feedback case in the absence of stochastic forcing. Because the precipitation forcing varies very slowly, the coupled climate-vegetation state almost coincides with a coupled equilibrium state during the evolution, a green state before −5500 yr and a desert state afterwards. Around −5500 yr, the coupled state collapses through an unstable collapse (UC). That is, the positive vegetation-climate feedback generates multiple equilibria in the coupled system, which allow a gradual insolation forcing to induce an abrupt collapse at −5500 yr from the green Sahara to a desert state via an unstable intermediate state [*Claussen et al.*, 1999]. In comparison, in the weak feedback case (Figures 4c and 4d), both the vegetation and precipitation exhibit much gradual declines from the green Sahara to a desert. This gradual decline will be called a stable decline (SD). In general, an UC occurs faster and with a larger rainfall decline than a SD. In our conceptual model, the duration for the vegetation to decrease from the green (V = 1) to desert (V = 0) states is:

$$\frac{\Delta t_{collapse}}{T_P} = \begin{cases} -(D_B - D_C)/P_{d0}, & D_B \le D_C,\ SD \\ 0, & D_B > D_C, UC \end{cases}$$

accompanied by a rainfall reduction of

$$\Delta P_{collapse} = \begin{cases} D_C, & D_B \le D_C, \quad SD \\ D_C + (D_B - D_C) \equiv D_B, & D_B > D_C, \quad UC. \end{cases}$$

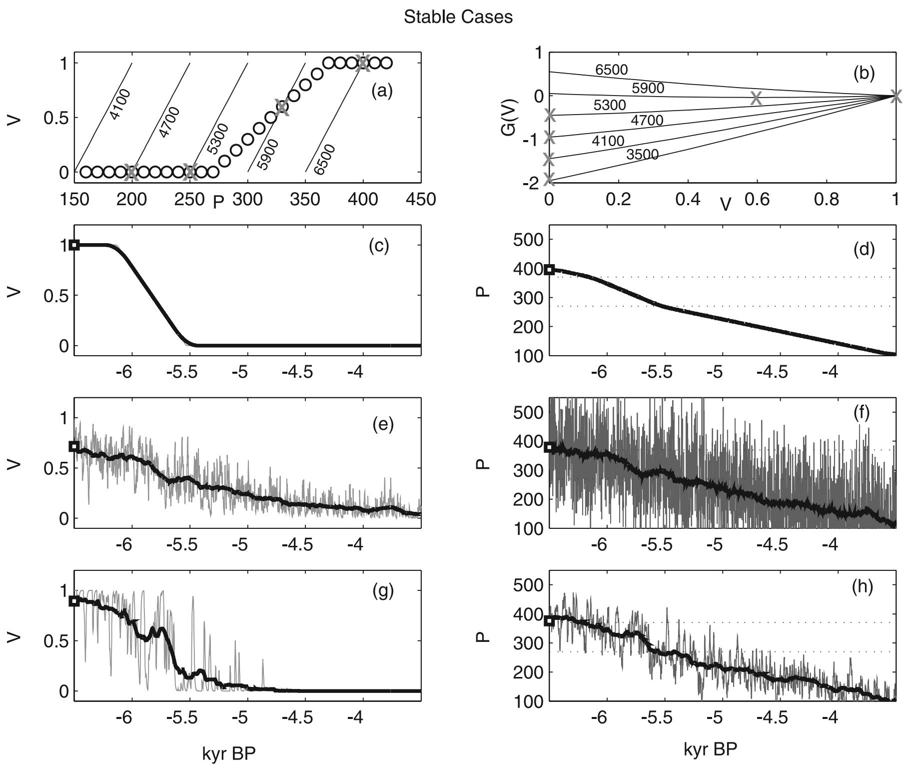

Figure 4. Vegetation-climate solution in the conceptual model for the weak feedback case. Same as Figure 3, except for D_B = 50 mm/yr. Here, Figures 4c and 4d show the stable decline, while 4g and 4h show the stable collapse excited by a slow stochastic forcing.

Therefore, in contrast to the instantaneous UC, SD occurs over a longer time for a less positive vegetation feedback and in turn more stable system (more negative $D_B - D_C$). Furthermore, the stronger the positive vegetation feedback, the more unstable the system (more positive $D_B - D_C$), and the greater the rainfall reduction is. In particularly, precipitation reduction is always larger in UC than in SD.

[8] The SD, we speculate, is responsible for the gradual decline in North African vegetation in the work by *Wang et al.* [2005]. This is because their model, albeit with the same vegetation model as *Claussen et al.* [1999], has neither strong climate variability, nor a strong vegetation feedback.

5. Suppression of Collapse by Fast Climate Variability

[9] Precipitation in southern Sahara exhibits substantial climate variability in our model (Figure 1c), and also in the real world. Here, we use a random annual precipitation $\overline{P}_N^{1\,\mathrm{yr}}$ with a standard deviation of 130 mm/yr. This climate variability is seen to suppress the UC in the strong feedback case (Figures 3e and 3f), in which the decline of climatological vegetation and rainfall (say, the 100-year running mean) becomes gradual, with no systematic abrupt collapse. This suppression of abrupt collapse can be understood as follows. Without stochastic forcing, the background forcing varies so slowly that the coupled climate-vegetation system evolves following the equilibrium state. Therefore, a coupled state tends to reside in either the stable green equilibrium, or the stable desert equilibrium, once it falls into each respective "attractive well" (Figure 3b). With a strong and fast stochastic forcing, the coupled system is driven frequently out of its attractive well into the other attractive well. Over a long time, this tends to generate an equal probability of residence near the two stable equilibria, and therefore an ensemble mean state in between the two equilibria. A similar situation has been studied in an ocean model [*Stommel and Young*, 1993] and a coupled vegetation-climate model of intermediate complexity [*Wang*, 2004]. In a sense, the climate variability forcing is so fast and so strong that the response can no longer "stick" around a stable equilibrium state. Instead, the coupled state "wanders" around the "center of gravity" of the two equilibria. As such, with a slowly evolving mean background forcing, there will be no longer a systematic sudden collapse from one equilibrium to another because the coupled system is no longer closely "attached" to any specific equilibrium at any time. This way, climate variability effectively smoothes the temporal evolution of the coupled system. Similarly, the coupled evolution is also smoothed by the stochastic forcing in the weak feedback case (Figures 4e and 4f). This smoothing effect on the temporal evolution of the coupled system is similar to the smoothing effect of climate variability on the spatial gradient between vegetation and desert [*Zeng and Neelin*, 2000]. The smoothing effect of climate variability, on both the temporal and spatial gradients in the coupled system, tends to counter the gradient-sharpening effect from positive vegetation-climate feedback.

[10] This stochastic suppression offers an explanation why northern Africa vegetation shows little abrupt collapse

of *Renssen et al.* [2003], in spite of their identical vegetation model to the one of *Claussen et al.* [1999]. Renssen et al. adopt a quasi-geostrophic atmospheric model, which may have produced excessive rapid synoptic climate noise, which then suppresses UC. Note here that, to suppress a collapse, the stochastic forcing has to be faster than the vegetation equilibrium time. A fast and strong forcing causes random vacillations of the coupled state between extreme states with no time to reach equilibrium, preventing a collapse of the coupled state.

6. Excitation of Collapse by Slow Climate Variability

[11] The coupled system evolves very differently under a slow stochastic forcing. Grasslands mainly depend on surface soil moisture, but they also have a weak dependence on subsurface moisture with a persistence time of decades. This is because perennial grasses, especially in seasonally dry tropical environments, also have a proportion of deep roots that can be crucial for their survival through the dry season. As such, subsurface soil moisture provides a long-term memory effect for grasses. The long-term effect can also be further enhanced by vegetation-climate interaction, which has been shown to enhance decadal low frequency variability in precipitation at the expense of shorter inter-annual variability [*Zeng et al.*, 1999]. These long-term effects of climate variability and soil moisture are here approximated crudely as a 10-year running mean of a stochastic annual precipitation forcing $\overline{P}_N^{10\ \mathrm{yr}}$.

[12] In the strong feedback case, the slow stochastic forcing reactivates the UC (Figures 3g and 3h). Unlike a fast stochastic forcing, the slow stochastic forcing has a persistence time comparable or longer than the vegetation equilibrium time. Thus, the coupled system can still follow closely to its equilibrium during the evolution before the stochastic forcing changes significantly. When the equilibrium state switches, the system collapses, leading to the UC.

[13] Most interestingly, in the weak feedback case, a slow stochastic forcing can excite a vegetation collapse (Figure 4g) accompanied by a weak precipitation decline (Figure 4h); this will be called a stable collapse (SC), which occurs much faster than the SD in the absence of stochastic forcing (Figures 4c and 4d). The mechanism of the SC may be understood as follows. In a coupled vegetation-climate system, both the green state and desert state have a broad and deep attractive well relative to the intermediate state (e.g., Figure 4b), because of the two nonlinear bioclimatic thresholds for vegetation: P_{C1} and P_{C2}. The green and desert states are therefore stable subject to large perturbations, as long as the perturbation does not vary too fast to allow for vegetation equilibration. Consequently, a system is easily driven out of the intermediate state by a moderate perturbation, leading to the SC. Similar to the SD, however, the precipitation collapse in the SC is much weaker than in the UC (Figure 4h vs. Figure 3h), because of the weak vegetation feedback. Finally, further experiments suggest that the timing of the collapse differs for each realization, and could vary substantially for both the stable and unstable collapses. Nevertheless, in both cases, vegetation tends to collapse when the climatological rainfall falls to around the rainfall thresholds P_{C2} and P_{C1}. This SC, we speculate, offers an explanation of the strong vegetation collapse accompanied by a gradual precipitation decline in FOAM-LPJ (Figures 1b and 1c).

7. Implications

[14] Our conceptual model study shows that the North African vegetation collapse during the mid-Holocene could have been caused either by a strong vegetation feedback as a UC, or by a strong low frequency climate variability as a SC. The former is accompanied by a strong collapse in precipitation, while the latter is not. The vegetation collapse in FOAM-LPJ (Figures 1b and 1c), we speculate, is caused by the SC, because of the weak vegetation feedback, strong rainfall variability, and the absence of an abrupt precipitation collapse. In contrast, the vegetation collapse of *Claussen et al.* [1999] is likely a UC, because of a weak stochastic forcing and strong positive vegetation feedback in their model.

[15] Our study has important implications to future modelling and observational studies. The simulated vegetation collapse depends not only on the vegetation model, but also on the climate model and climate-vegetation interactions. Furthermore, the vegetation collapse is determined not only by the mean climate and vegetation feedback, but also by climate variability. With strong climate variability, vegetation feedback becomes no longer essential for the vegetation collapse. It should also be pointed out that the potential role of climate variability on abrupt change discussed here may have important implications to abrupt changes in other climate system, such as the oceanic thermohaline circulation.

[16] In practice, it is important to clarify if the mid-Holocene collapse was caused by vegetation feedback as in UC, or by climate variability as in SC. In spite of various modeling studies [*Claussen*, 1997; *Kutzbach et al.*, 1996], there has been little direct observational evidence of a strong positive vegetation feedback on large-scale precipitation in northern Africa [*Liu et al.*, 2006]. In the Holocene, the sudden increase in dust flux at marine sediment cores likely reflects the dramatic vegetation collapse. However, there seems to be no clear evidence of an abrupt collapse in large-scale precipitation. Recent analysis of North Atlantic marine sediment suggests a gradual change in coastal upwelling and SST accompanying the sudden increase in dust flux in the mid-Holocene [*Adkins et al.*, 2006]. Therefore, the sudden increase in dust flux could be caused by a sudden replacement of grasses with desert, which would produce a rapid increase in dust transport towards the Atlantic despite a gradual change in wind and precipitation. This is consistent with the gradual precipitation change and abrupt vegetation change in the SC. To resolve this issue, high-resolution paleohydrology data are critically needed. If the reconstructed vegetation collapse is accompanied by an abrupt reduction of large scale hydrological cycle, the abrupt change is likely to be caused by the UC proposed by *Claussen et al.* [1999]. Otherwise, it is likely to be caused by the SC proposed here.

[17] **Acknowledgments.** We acknowledge the helpful discussions with F. Gasse, T. Johnson, P. deMenocal, J. Adkins and J. Kutzbach on the implication of paleo-climatic observations. We also thank the helpful

comments from M. Claussen and two anonymous reviewers. This work is supported by ESH/NSF. This work is CCR contribution number 910.

References

Adkins, J., P. deMenocal, and G. Eshel (2006), The "African humid period" and the record of marine upwelling from excess ^{230}Th in Ocean Drilling Program Hole 658C, *Paleoceanography*, *21*, PA4203, doi:10.1029/2005PA001200.

Berger, A. (1978), Long-term variation of daily insolation and Quaternary climatic changes, *J. Atmos. Sci.*, *35*, 2362–2367.

Brovkin, V., M. Claussen, V. Petoukhov, and A. Ganopolski (1998), On the stability of the atmosphere-vegetation system in the Sahara/Sahel region, *J. Geophys. Res.*, *103*(D24), 31,613–31,624.

Claussen, M. (1997), Modeling biogeophysical feedback in the African and Indian monsoon region, *Clim. Dyn.*, *13*, 247–257.

Clausen, M. (1998), On multiple solutions of the atmosphere-vegetation system in present-day climate, *Global Change Biol.*, *4*, 549–559.

Claussen, M., C. Kubatzki, V. Brovkin, A. Ganopolski, P. Hoelzmann, and H. Pachur (1999), Simulation of an abrupt change in Saharan vegetation in the mid-Holocene, *Geophys. Res. Lett.*, *26*, 2037–2040.

deMenocal, P., et al. (2000), Abrupt onset and termination of the African Humid Period: Rapid climate responses to gradual insolation forcing, *Quat. Sci. Rev.*, *19*, 347–361.

Gallimore, R., R. Jacob, and J. E. Kutzbach (2005), Coupled atmosphere-ocean-vegetation simulations for modern and mid-Holocene climates: Role of extratropical vegetation cover feedbacks, *Clim. Dyn.*, *25*, 755–776.

Kutzbach, J. E., G. Bonan, J. Foley, and S. P. Harrison (1996), Vegetation and soil feedbacks on the response of the African monsoon to orbital forcing in the early to middle Holocene, *Nature*, *384*, 623–626.

Liu, Z., M. Notaro, J. Kutzbach, and N. Liu (2006), Assessing global vegetation-climate feedbacks from the observation, *J. Clim.*, *19*, 787–814.

Renssen, H., V. Brovkin, T. Fichefet, and H. Goosse (2003), Holocene climate instability during the termination of the African Humid Period, *Geophys. Res. Lett.*, *30*(4), 1184, doi:10.1029/2002GL016636.

Stommel, H. M., and W. R. Young (1993), The average T-S relation of a stochastically forced box model, *J. Phys. Oceanogr.*, *23*, 151–158.

Wang, G. L. (2004), A conceptual modeling study on biosphere-atmosphere interactions and its implications for physically based climate modelling, *J. Clim.*, *17*, 2572–2583.

Wang, Y., L. A. Mysak, Z. Wang, and V. Brovkin (2005), The greening of the McGill Paleoclimate Model: Part II. Simulation of Holocene millennial-scale natural climate changes, *Clim. Dyn.*, *24*, 481–496.

Zeng, N., and J. D. Neelin (2000), The role of vegetation-climate interaction and interannual variability in shaping the African savanna, *J. Clim.*, *13*, 2665–2670.

Zeng, N., J. D. Neelin, K. M. Lau, and C. J. Tucker (1999), Enhancement of interdecadal climate variability in the Sahel by vegetation interaction, *Science*, *286*, 1537–1540.

R. Gallimore, Z. Liu, M. Notaro, and Y. Wang, Center for Climatic Research, University of Wisconsin-Madison, 1225 West Dayton Street, Madison, WI 53706, USA. (zliu3@wisc.edu)

I. C. Prentice, Department of Earth Sciences, University of Bristol, Queen's Road, Bristol BS8 1RJ, UK.